Original Article

Discovery of a novel calcium-sensitive fluorescent probe for α-ketoglutarate

Lin-lin GAN[1, 2], Lin-hai CHEN[1, 2], Fa-jun NAN[1, 2, *]

[1]Chinese National Center for Drug Screening, State Key Laboratory of Drug Research, Shanghai Institute of Materia Medica, Chinese Academy of Sciences, Shanghai 201203, China; [2]University of Chinese Academy of Sciences, Beijing 100049, China

Abstract

α-Ketoglutarate (α-KG), a pivotal metabolite in energy metabolism, has been implicated in nonalcoholic fatty liver disease (NAFLD) and several cancers. It is recently proposed that plasma α-KG is a surrogate biomarker of NAFLD. Here, we report the development of a novel "turn-on" chemosensor for α-KG that contains a coumarin moiety as a fluorophore. Using benzothiazole-coumarin (BTC) as inspiration, we designed a probe for calcium ion recognition that possesses a unique fluorophore compared with previously reported probes for α-KG measurement. This chemosensor is based on the specific Schiff base reaction and the calcium ion recognition property of the widely used calcium indicator BTC. The probe was synthesized, and a series of parallel experiments were conducted to optimize the chemical recognition process. Compared to the initial weak fluorescence, a remarkable 7.6-fold enhancement in fluorescence intensity (I/I_0 at 495 nm) was observed for the conditions in which the probe (1 μmol/L), α-KG (50 μmol/L), and Ca^{2+} (100 μmol/L) were incubated at 30 °C in EtOH. The probe displayed good selectivity for α-KG even in an environment with an abundance of amino acids and other interfering species such as glutaric acid. We determined that the quantitative detection range of α-KG in EtOH was between 5 and 50 μmol/L. Finally, probe in serum loaded with α-KG (10 mmol/L) showed a 7.4-fold fluorescence enhancement. In summary, a novel probe for detecting the biomarker α-KG through a typical Schiff base reaction has been discovered. With further optimization, this probe may be a good alternative for detecting the physiological metabolite α-KG.

Keywords: nonalcoholic fatty liver disease; biomarker; α-ketoglutarate; fluorescent probe; calcium-sensitive; benzothiazole-coumarin

Introduction

Small molecule biomarkers provide diagnostic insight into disease etiology or progression, and the detection of biomarkers plays an important role in the early diagnosis and treatment of diseases[1-6]. α-KG, also referred to as α-ketoglutaric acid, is a rate-determining intermediate in the tricarboxylic acid (TCA) cycle and plays a crucial role in cellular energy metabolism. Joven et al recently reported that plasma α-KG is a surrogate biomarker of NAFLD; thus, the direct measurement of α-KG may reduce the need for liver biopsies and may be useful in the assessment of disease progression and in the search for therapeutic options[7]. Additionally, mutated isocitrate dehydrogenase (IDH) transforms α-ketoglutarate (α-KG) into 2-hydroxyglutarate (2-HG), which is an oncometabolite in acute myeloid leukemia (AML) and glioma patients[8-14].

The most frequently used methods for analyzing α-KG are gas chromatography[15]/high-performance liquid chromatography-mass spectrometry[16] (GC/HPLC-MS). However, these methods are inconvenient because GC-MS and HPLC-MS both require tedious pretreatment. Accordingly, considerable research has focused on identifying fluorescent sensors that provide facile and sensitive methods to detect α-KG without requiring a bulky device[17, 18].

BTC is a low affinity calcium indicator (K_d=7 μmol/L) that exhibits an excitation wavelength shift from 462 nm to 401 nm upon binding Ca^{2+} with a fixed emission wavelength of 530 nm[19]. Its four carboxylic acid groups simulate the structure of ethylene glycol-bis(β-aminoethyl ether)-N,N,N',N'-tetraacetic acid (EGTA) and thus are believed to be involved in calcium chelation. Using BTC as inspiration, we designed a probe for calcium ion recognition that possesses a unique fluorophore for α-KG measurement. An intermediate with four carboxyl groups should be generated in situ from the probe and α-KG through a typical Schiff base reaction. This intermediate is similar to BTC and therefore may exhibit fluorescence changes that can be used to measure the concentration of α-KG (Figure 1).

The probe was synthesized in five steps, as outlined in Scheme 1. A series of parallel experiments was conducted to
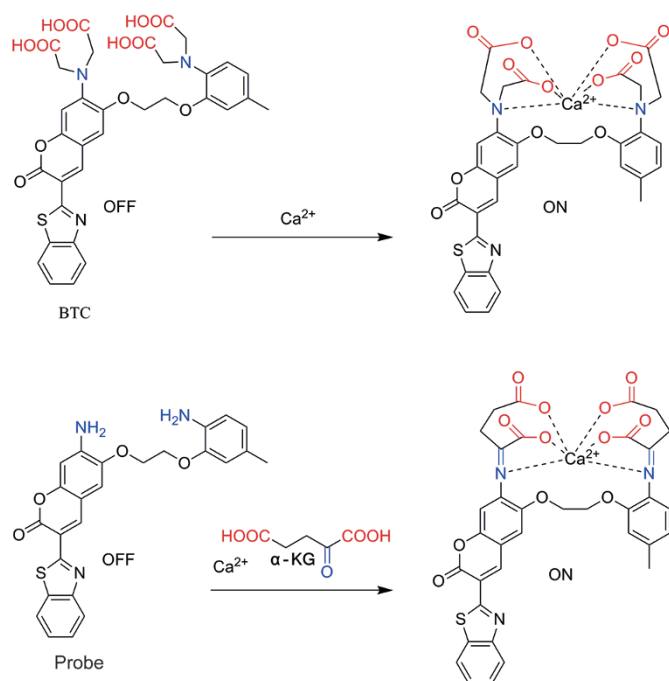
Figure 1. Rational design of probe for detecting α-KG.

optimize the chemical recognition process. The probe itself exhibited weak fluorescence with a maximum excitation wavelength of 439 nm and a maximum emission wavelength of 495 nm. When α-KG and Ca^{2+} were added to the system under optimum conditions, the emission fluorescence intensity was significantly enhanced, although no significant shift in the excitation or emission wavelength was observed.
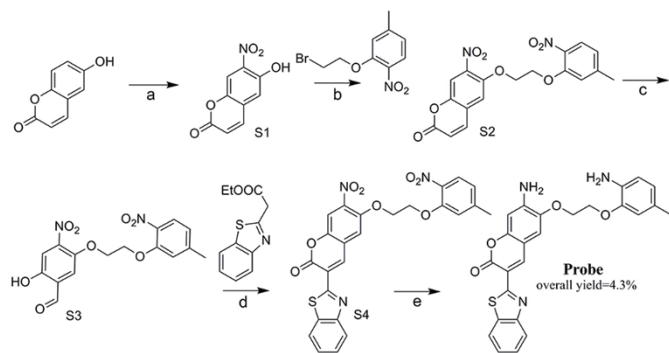
Scheme 1. Synthesis of probe.

Materials and methods
Chemistry
Starting materials, reagents, and solvents were purchased from commercial suppliers and used without further purification unless otherwise stated. All non-aqueous reactions were performed under an inert atmosphere (nitrogen or argon) with rigid exclusion of moisture from reagents, and all reaction ves-

sels were oven dried. 6-Hydroxycoumarin and ethyl 2-(2-benzothiazolyl)acetate were purchased from Tokyo Chemical Industry Co, Ltd (Shanghai). 2-(2-Bromoethoxy)-4-methyl-1-nitrobenzene was prepared according to the literature methods[20].

^{1}H NMR spectra were recorded on a spectrometer operating at 300 MHz with tetramethylsilane (TMS) as an internal reference. ^{13}C NMR spectra were recorded on a spectrometer operating at 125 MHz with tetramethylsilane (TMS) as an internal reference. HRMS were measured on an Agilent Accurate-Mass Time-of-Flight (TOF) LC/MS 6224 spectrometer. Reaction progress was monitored by silica gel thin layer chromatography (TLC) plates that were visualized under UV. Products were purified by flash column chromatography (FCC) on 200-300 mesh silica gel. The absorption spectra and emission spectra in solution were measured with a multifunctional SpectraMax M5 microplate reader.

Reagents and conditions
6-Hydroxy-7-nitro-2H-chromen-2-one (S1)
6-Hydroxycoumarin (6 g, 37.01 mmol) was suspended in dry MeCN (180 mL), a solution of ceric ammonium nitrate (2.03 g, 37.01 mmol) in dry MeCN (180 mL) was added via syringe, and the resulting mixture was stirred for 30 min at room temperature. Upon completion (monitored by TLC), all solid materials disappeared, and the reaction mixture became clear. The mixture was poured into ice water and extracted with EtOAc. The organic layer was washed sequentially with saturated sodium bisulfate and brine, dried over anhydrous Na_2SO_4, and concentrated in vacuo. The residue was further purified by silica gel column chromatography (CH_2Cl_2). Compound **S1** was obtained as a yellow solid (500 mg, 6.5%). ^{1}H NMR (300 MHz, $CDCl_3$): δ 10.29 (s, 1H), 8.08 (s, 1H), 7.67 (d, *J*=9.6 Hz, 1H), 7.28 (s, 1H), 6.62 (d, *J*=9.6 Hz, 1H). ^{13}C NMR (125 MHz, $CD_3OD+CDCl_3$): δ 159.58, 149.64, 145.03, 141.56, 135.27, 125.32, 119.95, 117.38, 112.00. HRMS (ESI) *m/z* calc'd for $C_9H_5NO_5$ [M-H]⁻ 206.0095, found 206.0262.

6-(2-(5-Methyl-2-nitrophenoxy)ethoxy)-7-nitro-2H-chromen-2-one (S2)
To a stirred solution of **S1** (500 mg, 2.41 mmol) in dry DMF (50 mL) was added 2-(2-bromoethoxy)-4-methyl-1-nitrobenzene (630 mg, 2.41 mmol), anhydrous potassium carbonate (500 mg, 3.62 mmol), and anhydrous KI (40 mg, 0.24 mmol), and the reaction mixture was stirred for 3 h at 70 °C. At this time, 2-(2-bromoethoxy)-4-methyl-1-nitrobenzene (630 mg, 2.41 mmol), anhydrous potassium carbonate (500 mg, 3.62 mmol), and anhydrous KI (40 mg, 0.24 mmol) were added, and the reaction mixture was stirred for another 2 h at 70 °C. After completion (monitored by TLC), the solution was acidified with 1 mol/L HCl, filtered, washed with water, and dried. The precipitated solid was further purified by silica gel column chromatography (petroleum ether/EtOAc=2/1). Compound **S2** was obtained as a yellow solid (831 mg, 89.1%). ^{1}H NMR (300 MHz, $CDCl_3$): δ 2.44 (s, 3H), 4.50 (t, *J*=3.9 Hz, 2H), 4.65 (t, *J*=3.9 Hz, 2H), 6.59 (d, *J*=9.6 Hz, 1H), 6.89 (d, *J*=8.4 Hz, 1H), 6.95 (s, 1H), 7.63 (s, 1H), 7.73 (s, 1H), 7.80 (d, *J*=8.1 Hz, 1H),

7.88 (d, *J*=9.6 Hz, 1H). ^{13}C NMR (125 MHz, CDCl$_3$): δ 159.52, 152.01, 148.53, 147.64, 146.56, 142.09, 142.00, 137.68, 126.18, 123.14, 122.24, 120.13, 116.02, 115.56, 113.71, 70.53, 69.15, 22.10. HRMS (ESI) *m/z* calc'd for C$_{18}$H$_{14}$N$_2$O$_8$ [M+H]$^+$ 387.0823, found 387.0822.

2-Hydroxy-5-(2-(5-methyl-2-nitrophenoxy)ethoxy)-4-nitrobenzaldehyde (S3)

Compound **S2** (831 mg, 2.15 mmol) was dissolved in CH$_2$Cl$_2$ (250 mL) and cooled to 0 °C. The reaction mixture was exposed to ozone for 1 h at 0 °C. After complete consumption of **S2** was observed (based on TLC), the reaction mixture was stirred overnight with excess dimethylsulfide at room temperature. The solution was then concentrated in vacuo and purified by silica gel column chromatography (petroleum ether/EtOAc=4/1 to 2/1). Compound **S3** was obtained as a yellow solid (700 mg, 89.9%). ^{1}H NMR (300 MHz, CDCl$_3$): δ 10.83 (s, 1H), 10.07 (s, 1H), 7.80 (d, *J*=8.4 Hz, 1H), 7.73 (s, 1H), 7.30 (s, 1H), 6.93 (s, 1H), 6.88 (d, *J*=7.5 Hz, 1H), 4.58 (t, *J*=3.9 Hz, 2H), 4.46 (t, *J*=3.9 Hz, 2H), 2.44 (s, 3H). ^{13}C NMR (125 MHz, CDCl$_3$): δ 196.30, 156.05, 152.07, 146.48, 146.43, 144.51, 137.74, 126.13, 122.75, 122.65, 122.15, 115.53, 113.99, 71.18, 69.04, 22.09. HRMS (ESI) *m/z* calc'd for C$_{16}$H$_{14}$N$_2$O$_8$ [M+H]$^+$ 363.0823, found 363.0823.

3-(Benzo[d]thiazol-2-yl)-6-(2-(5-methyl-2-nitrophenoxy)ethoxy)-7-nitro-2H-chromen-2-one (S4)

S3 (700 mg, 1.93 mmol) and ethyl 2-(2-benzothiazolyl)acetate (1.07 g, 4.83 mmol) were suspended in dry EtOH (180 mL), piperidine (860 µL, 8.70 mmol) was added via syringe, and the resulting mixture was refluxed overnight. After completion (monitored by TLC), the reaction mixture was poured into water and extracted with CH$_2$Cl$_2$. The organic layer was washed sequentially with saturated sodium bicarbonate and brine, dried over anhydrous Na$_2$SO$_4$, and concentrated in vacuo. The residue was further purified by silica gel column chromatography (petroleum ether/CH$_2$Cl$_2$=1/10). Compound **S4** was obtained as a yellow solid (560 mg, 56.00%). ^{1}H NMR (300 MHz, CDCl$_3$): δ 9.13 (s, 1H), 8.14 (d, *J*=8.4 Hz, 1H), 8.01 (d, *J*=8.1 Hz, 1H), 7.86 (s, 1H), 7.79 (d, *J*=8.4 Hz, 1H), 7.66 (s, 1H), 7.57 (t, *J*=7.2 Hz, 1H), 7.47 (t, *J*=7.2 Hz, 1H), 6.99 (s, 1H), 6.90 (d, *J*=7.8 Hz, 1H), 4.65 (t, *J*=3.9 Hz, 2H), 4.54 (t, *J*=3.9 Hz, 2H), 2.45 (s, 3H). ^{13}C NMR (125 MHz, *d*$_6$-DMSO): δ 159.14, 158.97, 151.95, 151.19, 146.95, 146.45, 145.77, 141.71, 139.97, 137.29, 136.24, 126.93, 125.87, 125.10, 122.84, 122.61, 122.42, 122.13, 121.57, 115.93, 115.46, 112.71, 68.69, 67.76, 21.33. HRMS (ESI) *m/z* calc'd for C$_{25}$H$_{17}$N$_3$O$_8$S [M+H]$^+$ 520.0809, found 520.0808.

7-Amino-6-(2-(2-amino-5-methylphenoxy)ethoxy)-3-(benzo[d]thiazol-2-yl)-2H-chromen-2-one (Probe)

To a stirred mixture of **S4** (20 mg, 0.04 mmol) and tetrabutyl ammonium bromide (38 mg, 0.12 mmol) was added anhydrous stannous chloride (44 mg, 0.23 mmol). The reaction mixture was stirred at room temperature until it became an ionic liquid. The liquid was then stirred for 4 h at 90 °C. After completion (monitored by TLC), the reaction was diluted

with water and extracted with CH$_2$Cl$_2$. The organic layer was washed with brine, dried over anhydrous Na$_2$SO$_4$, and concentrated in vacuo. The residue was further purified by silica gel column chromatography (petroleum ether/acetone=3/1). **Probe** was obtained as a yellow solid (10 mg, 55.56%). ^{1}H NMR (300 MHz, *d*$_6$-DMSO): δ 9.03 (s, 1H), 8.12 (d, *J*=7.5 Hz, 1H), 7.99 (d, *J*=8.1 Hz, 1H), 7.53 (t, *J*=9.6 Hz, 1H), 7.50 (s, 1H), 7.41 (t, *J*=7.8 Hz, 1H), 6.53 - 6.72 (m, 4H), 4.51 (s, 2H, NH), 4.40 (s, 2H), 4.36 (s, 2H), 2.27 (s, 3H). ^{13}C NMR (125 MHz, *d*$_6$-DMSO): δ 161.31, 160.29, 152.23, 152.15, 146.68, 145.32, 142.99, 142.64, 137.81, 135.35, 126.30, 125.09, 124.48, 121.98, 121.77, 121.68, 114.34, 113.59, 110.55, 110.37, 107.84, 97.89, 67.62, 66.74, 20.53. HRMS (ESI) *m/z* calc'd for C$_{25}$H$_{21}$N$_3$O$_4$S [M+H]$^+$ 460.1326, found 460.1326.

Biology

The detection of α-KG in fetal bovine serum was conducted according to previously reported methods[18]. In brief, 1 µmol/L probe and 10 mmol/L Ca^{2+} in EtOH (0.02% DMSO as cosolvent) were incubated with serum (loaded with α-KG, because the original content is very low) at 30 °C for 0.2 min, and the system was then centrifuged to separate the sediment. The fluorescence of the supernatant fraction was measured on a SpectraMax M5 multifunctional microplate reader.

Results
Probe design

BTC is a useful intracellular fluorescent probe for Ca^{2+}. Using the coumarin moiety as a fluorophore, the dye exhibits an excitation wavelength shift from 462 nm to 401 nm upon binding Ca^{2+}, whereas the emission wavelength of 530 nm remains unchanged. The quantum yield of this probe nearly doubles upon binding Ca^{2+}. The affinity of this probe for Ca^{2+} is low (K_d=7 µmol/L); therefore, it has an advantage over high affinity indicators for use in excitatory cells or extracellular spaces where calcium concentrations are very high[21].

Based on the structure of BTC and its calcium ion recognition, we designed a probe that employs a Schiff base reaction and exhibits remarkable spectral changes (Figure 1). The probe is a BTC derivative in which the substituents on the nitrogen atom are replaced by hydrogen atoms. The two amino groups of this probe act as specific recognition groups that react with the carbonyl group of α-KG to form the corresponding Schiff base product containing four carboxyl groups, which is similar to BTC. Upon chelating Ca^{2+}, the probe may exhibit fluorescence changes that can be used to determine the concentration of α-KG.

The yield and rate of Schiff base-generated reactions are known to be affected by various factors. To elicit the best possible fluorescent response during the chemical recognition process, optimum conditions for sensing α-KG were investigated. To optimize the recognition process, a variety of preliminary studies was performed, including optimization for the solvent, probe concentration, reaction temperature, and response time. The following experiments were conducted to identify conditions that would improve the fluorescent response to α-KG.

Probe synthesis

We explored synthetic pathways to the target molecule[22-24] and determined a simple and efficient route. Consisting of five steps, this route utilized 6-hydroxycoumarin as the starting material and gave the probe in an overall yield of 4.3% (Scheme 1). The structure of the probe was confirmed by NMR and MS analyses.

Solvent system optimization

To screen for an appropriate solvent, a series of parallel experiments was performed for the chemical recognition process. The probe was dissolved in DMSO to prepare a 5×10^{-3} mol/L stock solution and then diluted to 1×10^{-6} mol/L in various solvents, including tetrahydrofuran (THF), acetonitrile (MeCN), ethanol (EtOH), methanol (MeOH), dimethyl sulfoxide (DMSO), and H_2O. Except for the DMSO solution, these solutions contained 0.02% DMSO as a cosolvent.

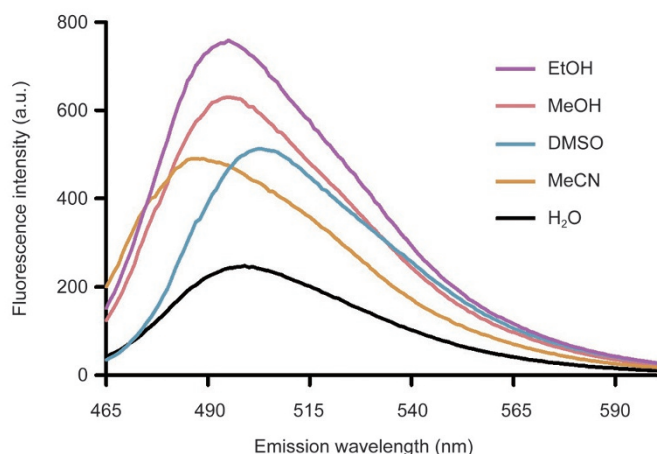Based on the spectra, we found that the probe had very

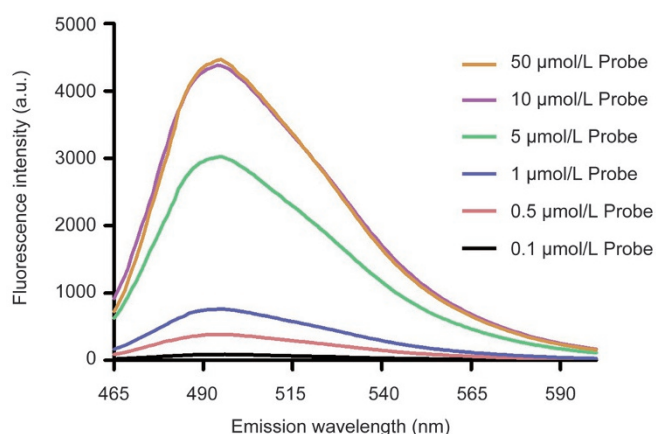**Figure 2.** Fluorescence intensity of probe (1 μmol/L) in different solvents; λ_{ex}=439 nm.

Figure 3. Probe concentration-dependent fluorescence intensity in ethanol; λ_{ex}=439 nm.

weak initial fluorescence in water but displayed stronger fluorescence in organic solutions (Figure 2). This result can be attributed to the hydrophobic structure of the probe and its higher solubility in organic solvents. Thus, in the following experiments, we chose EtOH as the best solvent for optimizing the fluorescent response for α-KG detection.

Probe concentration optimization

The probe concentration was predicted to have a significant influence on the fluorescence response. A series of experiments was conducted with the probe concentration ranging from 0.1 to 50 μmol/L. A low probe concentration did not produce sufficiently strong fluorescence for testing, and fluorescence quenching occurred at a probe concentration of 50 μmol/L (Figure 3). The suitable probe concentration, as a key characteristic of the kinetics affecting the reaction rate for the formation of Schiff base, was determined to be 1 μmol/L.

Temperature optimization

The relationship of the temperature to the kinetics of the reaction is also of major importance for the specific Schiff base reaction and thus was carefully investigated in the chemical recognition process. At temperatures of 30, 35, 40, and 45 °C, the fluorescence enhancement was 7.6, 6.3, 5.7, and 5.1, respectively (Figure 4A).

Although human physiological body temperature is approximately 37.5 °C, the experimental measurements showed that the greatest fluorescence enhancement was obtained at 30 °C. Furthermore, the fluorescence intensity decreased gradually with temperature. Therefore, 30 °C was chosen as the optimum temperature in the following experiments.

Response time optimization

For a reaction-based sensor, the response time plays an important role in the chemical recognition process. To confirm the appropriate response time of the reaction, we studied the reaction decay kinetics of the probe with α-KG and Ca^{2+} using a time-based fluorescence assay with response times of 0.2, 5, 10, 15, 20, 25, 30, 35, and 40 min.

Within 0.2 min, the fluorescence intensity of the probe increased significantly at 495 nm upon the addition of α-KG and Ca^{2+} in EtOH at 30 °C (Figure 4B). The experimental data revealed that the Schiff base reaction and chelation between calcium and the Schiff base product were completed instantaneously. Thus, 0.2 min was chosen as a suitable response time for the chemical recognition process.

Response to α-KG or Ca^{2+} alone

Because three components (probe, α-KG, and Ca^{2+}) were involved in our design strategy for α-KG analysis, we first investigated the fluorescent response of each factor. In the following tests in which elevated concentrations of α-KG or Ca^{2+} were added to an ethanol solution of the probe, we attempted to determine whether α-KG or Ca^{2+} would individually affect the emission fluorescence intensity.

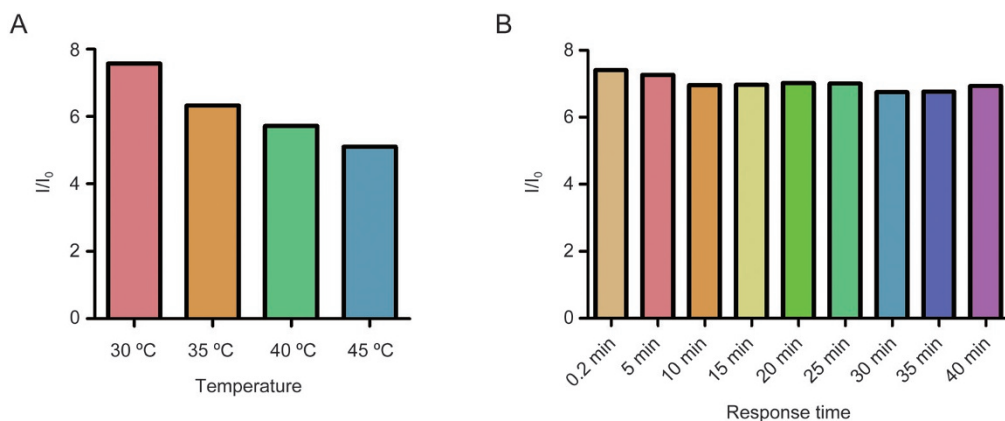There was only a subtle response of the probe to the addi-

A

B

Figure 4. (A) Fluorescent response of the probe (1 µmol/L) with α-KG (50 µmol/L) and Ca^{2+} (100 µmol/L) in ethanol after 0.2 min at different temperatures; (B) Fluorescent response of the probe (1 µmol/L) with α-KG (50 µmol/L) and Ca^{2+} (100 µmol/L) in ethanol at 30 °C after different times; I_0 and I represent the emission intensity of the probe at 495 nm in the absence (I_0) and presence (I) of α-KG and Ca^{2+}; λ_{ex}=439 nm.

A

B
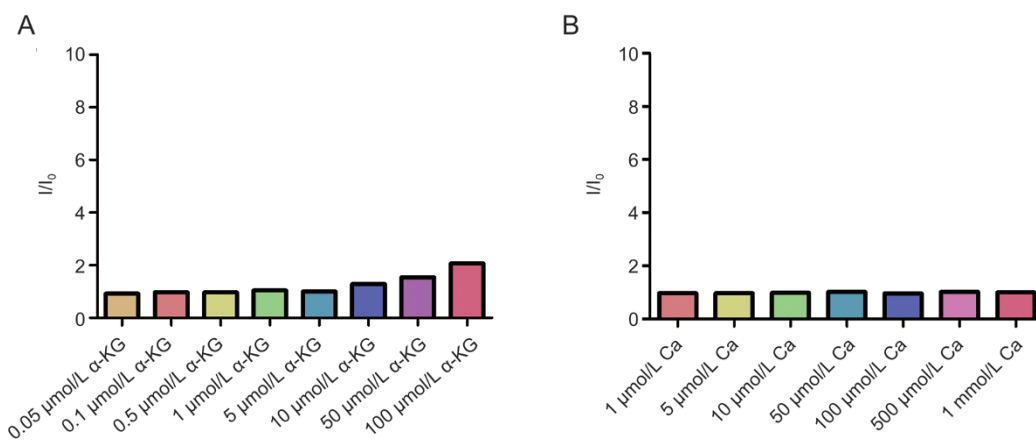
Figure 5. (A) Fluorescent response of the probe (1 µmol/L) with various α-KG concentrations in ethanol after 0.2 min at 30 °C; I_0 and I represent the emission intensity of the probe at 495 nm in the absence (I_0) and presence (I) of α-KG; (B) Fluorescent response of the probe (1 µmol/L) with various Ca^{2+} concentrations in ethanol after 0.2 min at 30 °C; I_0 and I represent the emission intensity of the probe at 495 nm in the absence (I_0) and presence (I) of Ca^{2+}; λ_{ex}=439 nm.

tion of different concentrations of Ca^{2+}, whereas the emission fluorescence intensity increased 1.5/2.1-fold upon the addition of a high concentration of α-KG (50 µmol/L/100 µmol/L) (Figure 5). Consistent with our assumption, the Schiff base product was formed between the probe and α-KG, and then responded to Ca^{2+} to produce a change in the fluorescence. Furthermore, Ca^{2+} did not elicit a response in the absence of α-KG.

Response to α-KG and Ca^{2+}

After completing the single factor parallel tests, we conducted a series of experiments on the system consisting of all three components. To verify our hypothesis regarding the chemical recognition process for α-KG detection, many possibilities were investigated by adding different concentrations of α-KG and Ca^{2+} simultaneously.

The most remarkable 4.9-fold fluorescence enhancement (the ratio of fluorescence with and without 100 µmol/L Ca^{2+}) at

495 nm occurred only when the concentrations of both α-KG (50 µmol/L) and Ca^{2+} (100 µmol/L) were very high (Figure 6). Because the affinity of BTC for Ca^{2+} is low (K_d=7 µmol/L), the high fluorescence increase with a high concentration of calcium is understandable. Furthermore, the significant response cannot be attributed to acidity because other combinations of components with 50 µmol/L α-KG exhibited a significantly smaller (1.5-fold) fluorescence enhancement. The interaction between the Schiff base product and calcium and the Schiff base chemical reaction itself were likely responsible for this interesting experimental result.

Selectivity of α-KG, various amino acids, pyruvic acid, and glutaric acid

A living cell is a delicate system that contains many complex components, such as amino acids and pyruvic acid. Therefore, we investigated the probe's selectivity in the presence of various amino acids. The probe's carbonyl selectivity was exam-
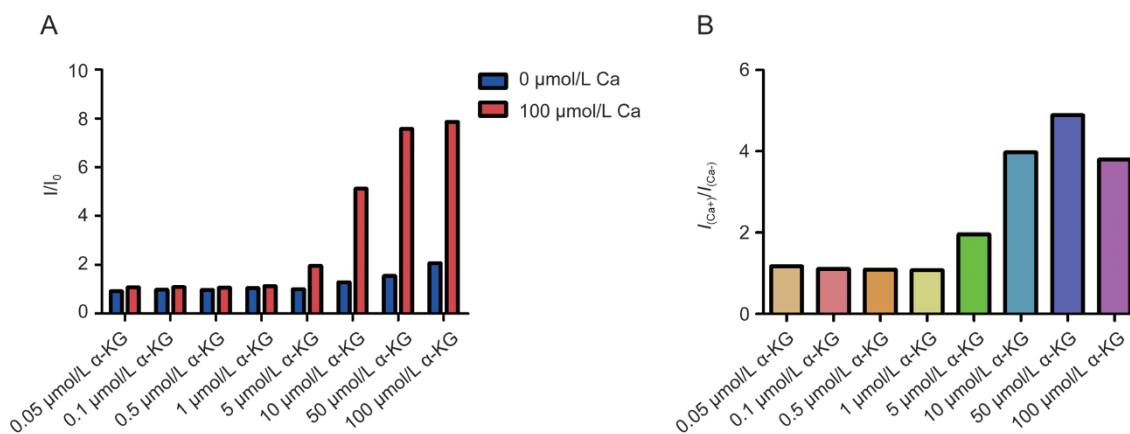
A

B

Figure 6. Fluorescent response of the probe (1 µmol/L) with α-KG (50 µmol/L) and Ca^{2+} (100 µmol/L) in ethanol after 0.2 min at 30 °C; λ_{ex}=439 nm. (A) I_0 and I represent the emission intensity of the probe at 495 nm in the absence (I_0) and presence (I) of α-KG and Ca^{2+}; (B) $I_{(Ca-)}$ and $I_{(Ca+)}$ represent the emission intensity of the probe at 495 nm in the absence ($I_{(Ca-)}$) and presence ($I_{(Ca+)}$) of Ca^{2+}.
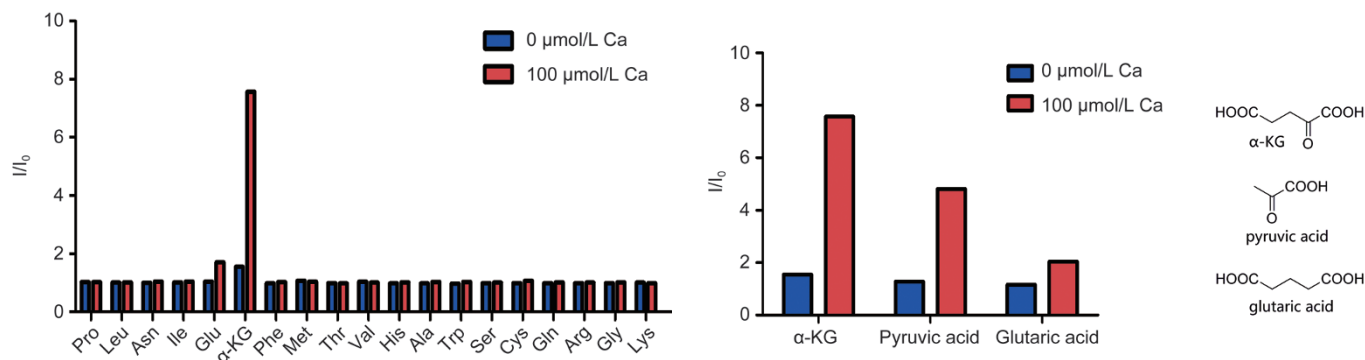

Figure 7. Fluorescent response of the probe (1 µmol/L) with α-KG/ different amino acids (50 µmol/L) and Ca^{2+} (100 µmol/L) in ethanol after 0.2 min at 30 °C; λ_{ex}=439 nm; I_0 and I represent the emission intensity of the probe at 495 nm in the absence (I_0) and presence (I) of α-KG/different amino acids and Ca^{2+}.
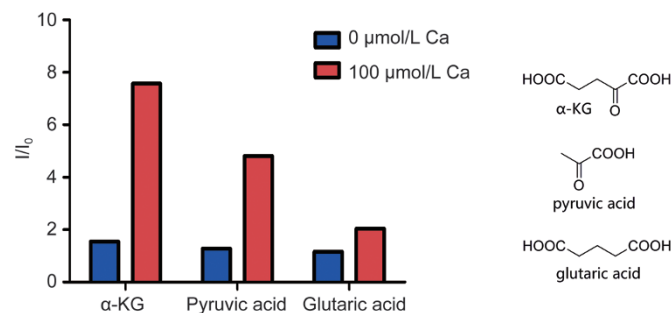

Figure 8. Fluorescent response of the probe (1 µmol/L) with α-KG/pyruvic acid/glutaric acid (50 µmol/L) and Ca^{2+} (100 µmol/L) in ethanol after 0.2 min at 30 °C; λ_{ex}=439 nm; I_0 and I represent the emission intensity of the probe at 495 nm in the absence (I_0) and presence (I) of α-KG/pyruvic acid/glutaric acid and Ca^{2+}.

ined under the optimum conditions; the probe (1 µmol/L) was tested with α-KG or various amino acids (50 µmol/L) at 30 °C in EtOH. Clearly, only α-KG caused a remarkable response with an approximately 7.6-fold fluorescence intensity increase at 495 nm (Figure 7). This result indicates that the probe exhibited good specificity toward α-KG even in an environment with an abundance of amino acids.

We also investigated two other potential competitors, pyruvic acid and glutaric acid, which have similar carbonyl and carboxyl groups as α-KG. Only α-KG exhibited a significant 7.6-fold fluorescence enhancement under the optimum conditions, whereas the other two compounds exhibited minor responses (Figure 8). This result was likely due to the lower reactivities of pyruvic acid and glutaric acid compared to α-KG, although these competitors could react with the probe. However, the response of the probe to pyruvic acid (approximately 5-fold) is greater than half that to α-KG (7.6-fold), indicating that it could interfere in α-KG detection. Further

optimization is ongoing.

Detection range in EtOH

With the knowledge that the probe is capable of selectively detecting α-KG in a complicated environment under optimum conditions, we conducted further studies to determine its detection range. By performing nonlinear curve fitting of the maximum fluorescence intensity of the probe with different α-KG concentrations, we obtained an S-curve in which the fluorescence intensity differed with changing α-KG concentrations. The quantitative detection range of α-KG was 5 µmol/L to 50 µmol/L with a probe concentration of 1 µmol/L and a calcium concentration of 100 µmol/L (Figure 9).

Potential application

Finally, considering its good performance under optimum conditions, the probe was used to detect α-KG in serum according to previously reported methods[18]. Due to the poor solubility
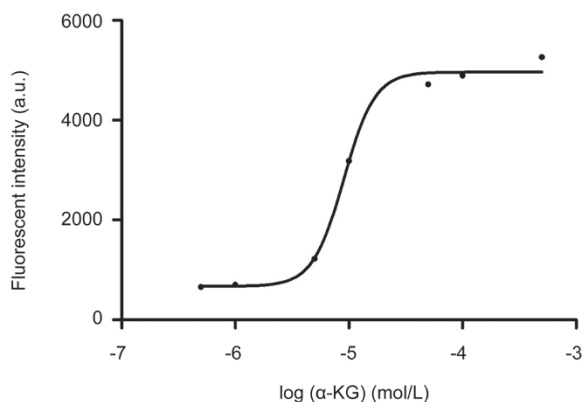
Figure 9. Detection range of α-KG.

Figure 10. Detection of α-KG in serum. Fluorescent response of the probe (1 µmol/L) in serum loaded with/without α-KG (100 µmol/L, 500 µmol/L, 1 mmol/L, 5 mmol/L, 10 mmol/L) and Ca^{2+} (10 mmol/L) in ethanol after 0.2 min at 30 °C; λ_{ex}=439 nm.

of the probe in water, 1 µmol/L probe and 10 mmol/L Ca^{2+} in ethanol were added into serum (loaded with α-KG, because the original level is very low). The system was then centrifuged to separate the sediment, and the supernatant fraction caused the most significant 7.4-fold fluorescence enhancement (Figure 10). Although the response was obtained with a high concentration of α-KG, a fluorescence response of our probe to α-KG occurred in the serum environment. Compared with the best solvent EtOH, the sensitivity of probe in serum decreased significantly, which is understandable considering the following: 1) serum containing various constituents is far more complicated than single solvent, and something in the serum may interfere with the probe's response to α-KG; 2) unlike organic solvent, the solubility of the probe was poor in aqueous systems, which limited our ability to improve sensitivity by increasing probe concentration. Further studies to improve the sensitivity of probe for α-KG in serum or other biological samples are currently in progress.

Discussion

Because elaborate pretreatment is essential for GC/LC-MS, these measurement methods that are most commonly used for α-KG need to be improved. Guo's group[17, 18] recently reported two fluorescent probes for α-KG. In the first probe, a hydrazino group was introduced into a naphthalimide moiety as the reaction trigger for the specific fluorescence turn-on response, and a diazanyl group was employed as the recognition group linked to a benzothiadiazole fluorophore moiety in their next sensor, DT.

In this work, a novel probe based on the typical Schiff base reaction was designed and synthesized for detecting the biomarker α-KG. In the specific chemical recognition process, ketimines were generated and then formed a calcium chelate via the four carboxyl groups. Notably, compared with the initial weak fluorescence intensity, a remarkable 7.6-fold enhancement (I/I_0 at 495 nm) was observed for conditions in which the probe (1 µmol/L), α-KG (50 µmol/L), and Ca^{2+} (100 µmol/L) were incubated for 0.2 min at 30 °C in EtOH. The chemical reaction in a system composed of the probe,
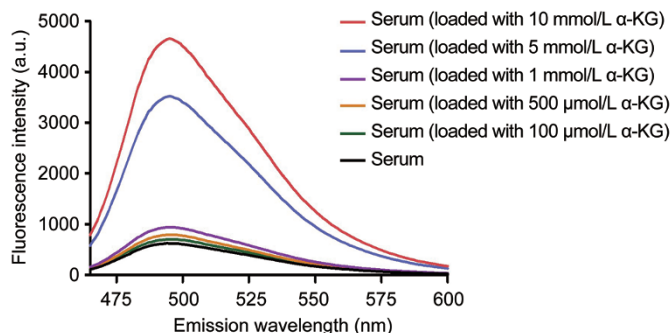
α-KG, and calcium is clearly responsible for the significant fluorescence increase because the two-component system of the probe and α-KG or Ca^{2+} was not responsive. Further studies showed that the probe displayed good selectivity towards α-KG even in an environment with an abundance of amino acids and other competitors. We also determined that the quantitative detection range of α-KG in EtOH was 5 µmol/L to 50 µmol/L. Finally, probe in serum loaded with 10 mmol/L α-KG was found to cause a most significant 7.4-fold fluorescence enhancement.

Considering that commercial kits detecting α-KG in patients are not available, our discovery of a fluorescent probe, although preliminary, is instructive for the development of α-KG sensors. With further optimization, our probe containing a fluorophore of BTC may be an alternative tool for detecting the physiological metabolite α-KG.

References

1 Chen J, Zeng L, Xia T, Li S, Yan T, Wu S, et al. Toward a biomarker of oxidative stress: a fluorescent probe for exogenous and endogenous malondialdehyde in living cells. Anal Chem 2015; 87: 8052–6.

2 Wang T, Douglass EF Jr, Fitzgerald KJ, Spiegel DA. A "turn-on" fluorescent sensor for methylglyoxal. J Am Chem Soc 2013; 135: 12429–33.

3 Xu J, Zhang Y, Zeng L, Liu J, Kinsella JM, Sheng R. A simple naphthalene-based fluorescent probe for high selective detection of formaldehyde in toffees and HeLa cells via aza-Cope reaction. Talanta 2016; 160: 645–52.

4 Yuen LH, Saxena NS, Park HS, Weinberg K, Kool ET. Dark hydrazone fluorescence labeling agents enable imaging of cellular aldehydic load. ACS Chem Biol 2016; 11: 2312–9.

5 Xu QY, Liu YH, Zhang Q, Ma B, Yang ZD, Liu L, et al. Metabolomic analysis of simvastatin and fenofibrate intervention in high-lipid diet-induced hyperlipidemia rats. Acta Pharmacol Sin 2014; 35: 1265–73.

6 Guo W, Cheng ZY, Zhu YZ. Hydrogen sulfide and translational medicine. Acta Pharmacol Sin 2013; 34: 1284–91.

7 Rodríguez-Gallego E, Guirro M, Riera-Borrull M, Hernández-Aguilera A, Mariné-Casadó R, Fernández-Arroyo S, et al. Mapping of the circulating metabolome reveals α-ketoglutarate as a predictor of morbid obesity-associated non-alcoholic fatty liver disease. Int J Obes 2015; 39: 279–87.

8 Dang L, White DW, Gross S, Bennett BD, Bittinger MA, Driggers EM, *et al*. Cancer-associated IDH1 mutations produce 2-hydroxyglutarate. Nature 2009; 462: 739–44.

9 Dang L, Yen K, Attar EC. IDH mutations in cancer and progress toward development of targeted therapeutics. Ann Oncol 2016; 27: 599–608.

10 Li F, He X, Ye D, Lin Y, Yu H, Yao C, *et al*. NADP$^+$-IDH mutations promote hypersuccinylation that impairs mitochondria respiration and induces apoptosis resistance. Mol Cell 2015; 60: 661–75.

11 Lu C, Ward PS, Kapoor GS, Rohle D, Turcan S, Abdel-Wahab O, *et al*. IDH mutation impairs histone demethylation and results in a block to cell differentiation. Nature 2012; 483: 474–8.

12 Zhao SM, Lin Y, Xu W, Jiang WQ, Zha ZY, Wang P, *et al*. Glioma-derived mutations in IDH1 dominantly inhibit IDH1 catalytic activity and induce HIF-1a. Science 2009; 324: 261–5.

13 Turcan S, Rohle D, Goenka A, Walsh LA, Fang F, Yilmaz E, *et al*. IDH1 mutation is sufficient to establish the glioma hypermethylator phenotype. Nature 2012; 483: 479–83.

14 Ye D, Xiong Y, Guan KL. The mechanisms of IDH mutations in tumorigenesis. Cell Res 2012; 22: 1102–4.

15 Nguyen DT, Lee G, Paik MJ. Keto acid profiling analysis as ethoxime/tert-butyldimethylsilyl derivatives by gas chromatography-mass spectrometry. J Chromatogr B Analyt Technol Biomed Life Sci 2013; 913-914: 48–54.

16 Tan B, Lu Z, Dong S, Zhao G, Kuo MS. Derivatization of the tricarboxylic acid intermediates with O-benzylhydroxylamine for liquid chromatography-tandem mass spectrometry detection. Anal Biochem 2014; 465: 134–47.

17 He Y, Guo Z, Jin P, Jiao C, Tian H, Zhu W. Optimizing the chemical recognition process of a fluorescent chemosensor for α-ketoglutarate. Ind Eng Chem Res 2015; 54: 2886–93.

18 Jin PW, Jiao CH, Guo ZQ, He Y, Zhu SQ, Tian H, *et al*. Rational design of a turn-on fluorescent sensor for a-ketoglutaric acid in a microfluidic chip. Chem Sci 2014; 5: 4012–6.

19 Hyrc KL, Bownik JM, Goldberg MP. Neuronal free calcium measurement using BTC/AM, a low affinity calcium indicator. Cell Calcium 1998; 24: 165–75.

20 Matsui A, Umezawa K, Shindo Y, Fujii T, Citterio D, Oka K, *et al*. A near-infrared fluorescent calcium probe: a new tool for intracellular multicolour Ca^{2+} imaging. Chem Commun 2011; 47: 10407–9.

21 Iatridou H, Foukaraki E, Kuhn MA, Marcus EM, Haugland RP, Katerinopoulos HE. The development of a new family of intracellular calcium probes. Cell Calcium 1994; 15: 190–8.

22 De P. Efficient reductions of nitroarenes with SnCl$_2$ in ionic liquid. Synlett 2004; (10): 1835–37.

23 Ganguly NC, Datta M, De P, Chakravarty R. Studies on regioselectivity of nitration of coumarins with cerium(IV) ammonium nitrate: solid-state nitration of 6-hydroxy-coumarins on montmorillonite K-10 clay support under microwave irradiation. Synthetic Commun 2003; 33: 647–59.

24 Bethke J, Margaretha P. Site selectivity in [2+2] photocycloadditions of tricyclic 'diethenylbenzenes' to 2,3-dimethylbut-2-ene. Helv Chim Acta 2002; 85: 544–51.